Aortic shape variation after frozen elephant trunk procedure predicts aortic events: Principal component analysis study

Check for updates

Michal Schäfer, PhD,[a] Adam Carroll, MD,[b] Kody K. Carmody, MS,[a] Kendall S. Hunter, PhD,[c] Alex J. Barker, PhD,[c,d] Muhammad Aftab, MD,[e] and T. Brett Reece, MD[e]

ABSTRACT

Objective: The frozen elephant trunk procedure is a well-established technique for the repair of type A ascending aortic dissection and complex aortic arch pathology. The ultimate shape created by the repair may have consequences in long-term complications. The purpose of this study was to apply a machine learning technique to comprehensively describe 3-dimensional aortic shape variations after the frozen elephant trunk procedure and associate these variations with aortic events.

Methods: Computed tomography angiography acquired before discharge of patients (n = 93) who underwent the frozen elephant trunk procedure for type A ascending aortic dissection or ascending aortic arch aneurysm was preprocessed to yield patient-specific aortic models and centerlines. Aortic centerlines were subjected to principal component analysis to describe principal components and aortic shape modulators. Patient-specific shape scores were correlated with outcomes defined by composite aortic event, including aortic rupture, aortic root dissection or pseudoaneurysm, new type B dissection, new thoracic or thoracoabdominal pathologies, residual descending aortic dissection with residual false lumen flow, or thoracic endovascular aortic repair complications.

Results: The first 3 principal components accounted for 36.4%, 26.4%, and 11.6% of aortic shape variance, respectively, and cumulatively for 74.5% of the total shape variation in all patients. The first principal component described variation in arch height-to-length ratio, the second principal component described angle at the isthmus, and the third principal component described variation in anterior-to-posterior arch tilt. Twenty-one aortic events (22.6%) were encountered. The degree of aortic angle at the isthmus described by the second principal component was associated with aortic events in logistic regression (hazard ratio, 0.98; 95% confidence interval, 0.97-0.99; $P = .046$).

Conclusions: The second principal component, describing angulation at the region of the aortic isthmus, was associated with adverse aortic events. Observed shape variation should be evaluated in the context of aortic biomechanical properties and flow hemodynamics. (JTCVS Open 2023;14:26-35)

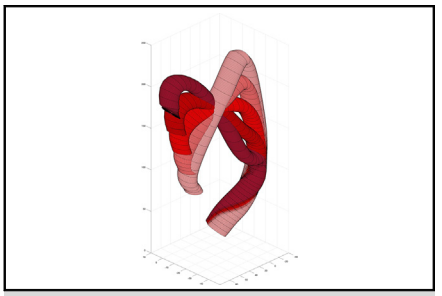

Aortic shape variation post-FET is associated with aortic events.

CENTRAL MESSAGE

Aortic shape post-FET repair with an acute angle at the isthmus is associated with adverse aortic events.

PERSPECTIVE

Complexity of the aortic shape after FET can be evaluated using PCA. The PC2, describing angulation at the region of the aortic isthmus, was associated with adverse aortic events. Observed shape variation might aid in demonstrating shape-dependent outcomes and should be evaluated in the context of aortic biomechanical properties and flow hemodynamics.

The frozen elephant trunk (FET) procedure is a well-established technique for the repair of type A acute aortic dissection (TAAAD) with the goal to achieve residual false lumen (FL) thrombosis and induce favorable aortic wall remodeling.[1] Improvements in the technique and perioperative management have significantly reduced surgical and acute phase mortality.[2] Currently, adverse aortic events including rupture or degeneration of residual dissection necessitating further surgical or endovascular procedure represent the major cause of mid- to long-term clinical complications.[3-5] Therefore, comprehensive imaging surveillance is critical in patients who underwent the FET technique for type A aortic dissection or ascending aortic aneurysm.

From the [a]Division of Cardiology, Heart Institute, [d]Department of Radiology, Children's Hospital Colorado; Departments of [b]Surgery, [c]Bioengineering, and [e]Division of Cardiothoracic Surgery, University of Colorado Denver Anschutz Medical Campus, Denver, Colo.

The study was approved by the University of Colorado Institutional Review Board with waived written consent, COMIRB #17 to 0198, approval date February 6, 2017.

Received for publication Dec 8, 2022; accepted for publication Jan 26, 2023; available ahead of print January 31, 2023.

Address for reprints: Michal Schäfer, PhD, Division of Cardiology, Heart Institute, Children's Hospital Colorado, 13123 E 16th Ave, Aurora, CO 80045-2560 (E-mail: michal.schafer@cuanschutz.edu).

2666-2736

Copyright © 2023 The Author(s). Published by Elsevier Inc. on behalf of The American Association for Thoracic Surgery. This is an open access article under the CC BY-NC-ND license (http://creativecommons.org/licenses/by-nc-nd/4.0/).

https://doi.org/10.1016/j.xjon.2023.01.015

Abbreviations and Acronyms

FET = frozen elephant trunk
FL = false lumen
PC = principal component
PCA = principal component analysis
SE = standard error
TAAAD = type A acute aortic dissection
TL = true lumen

Numerous studies have investigated the aortic remodeling post-FET repair in terms of 2- or 3-dimensional true lumen (TL) and FL geometric measurements, the degree of FL thrombosis, and intimal tear specifications.[6,7] Aortic shape is another marker of postsurgical remodeling frequently investigated in congenital heart disease in relation to cardiac loading conditions and resulting flow hemodynamics.[8-10] The FET procedure typically results in altered configuration of aortic shape and inelasticity of the central aorta.[11] Surgically modified aortic shape also tends to alter flow-mediated wall shear forces affecting the aortic wall remodeling and FL hemodynamic state.[12-14] Last, specific aortic shapes and flow hemodynamic interactions have been recently associated with the risk of development of TAAAD.[15] Aortic shape is often described by diameter measurements or qualitative descriptions such as "angular" or gothic arch.[16] However, substantial variability in aortic shape exists after the FET procedure because of the extent of aortic disease, tissue mechanics of the flap, nonuniformly dilated aortic wall, and even the structural differences between aortic tissue, fabric graft, and reinforced stent used distally.

Consequently, the purpose of this study was to apply principal component analysis (PCA), an unbiased machine learning technique, to quantitatively describe 3-dimensional aortic shape variation post-FET procedure. We further sought to investigate whether observed shape variations or their combinations are associated with aortic events. Specifically, we hypothesized that significant variation would exist in resulting aortic shape after the procedure and that these variations will be associated with the incidence of aortic events.

MATERIALS AND METHODS

As a part of a larger institutional study investigating the clinical outcomes in aortic surgery, we identified 93 patients who underwent the FET procedure between July 2016 and November 2021 for TAAAD or ascending aortic arch aneurysm. Included patients underwent initial postoperative scan before discharge from the hospital or within 1 month from the time of surgery. All selected patients underwent an institutionally modified version of the FET, the Buffalo technique, a modification obviating the need for commercially available hybrid graft as described previously.[17] The study was approved by the University of Colorado Institutional Review Board with the waived written consent because the study retrospectively collected from an institutionally approved database of all patients undergoing cardiac surgery (COMIRB #17-0198, approval date February 6, 2017).

Aortic Segmentation and Preprocessing

Postoperative imaging protocol included thin-sliced computed tomography angiography with triple-phase protocol. The work-flow diagram depicting aortic contour segmentation from the computed tomography angiography and preprocessing for further analysis is portrayed in Figure 1. Rough aortic contours were semiautomatically segmented in free open source software 3D Slicer (version 4.11.2 or higher).[18] To standardize aortic contours, the aortic lumen was segmented from the level of sinotubular junction proximally to the diaphragmatic level distally. Arch vessels or residual graft branches were removed. Last, only TL was considered for the aortic segmentation to limit the variability of residual FL. This step is primarily motivated by the need for the objective standardization of the input datasets before PCA analysis, which must be anatomically and demographically standardized (eg, curvature start and end points, patient size) for objective comparison or resulting shape vectors. FL parameters including its starting and terminal points, variable luminal patency, extent of thrombosis, and even communication with TL introduce variables difficult to standardize into a single unified vector representing curvature or single lumen shape. In the final preprocessing step, prepared and trimmed aortic contours were smoothed using Gaussian filter to remove residual surface irregularities and stent-graft imprints. The 3-dimensional aortic segmentations were then transformed to a surface model.

To study 3-dimensional variation of the aortic contour defined by primarily by its curvature, we proceeded with the aortic centerline analysis given the minimal radial variability as dictated by the presence of sewn grafts and stent-grafts. Centerlines were generated using built-in Vascular Modeling Toolkit module in 3D slicer from the created surface model between embedded fiducial points centered at proximal and distal ends of aortic model. Finalized centerline model yielded iterative data points along the centerline curve with 3-dimensional x, y, z coordinates with corresponding distance along the aortic centerline.

Before PCA, all aortic centerlines were preprocessed in MATLAB (Mathworks, Inc). Preprocessing involved 3 individual sequential steps: scaling, interpolation, and Procrustes analysis. First, all individual centerlines were scaled to mean centerline length of the considered patient population to limit variations in patient size and age. Second, each centerline was interpolated to generate 100 evenly spaced points. Last, Procrustes analysis was performed to determine an ideal linear transformation (translation, reflection, orthogonal rotation) of the individual centerline points to best conform them to the general population mean centerline shape and location.

Principal Component Analysis of Aortic Shape

PCA is an unbiased machine learning method used for dimensionality reduction that converts a set of potentially correlated variables (individual data points along the aortic centerline) and convert them into a set of new vectors known as principal components (PCs) by the degree of variance explained. In other words, PCA seeks to identify underlying patterns in the collected set of aortic centerlines and describes them in terms of a smaller number of parameters (PCs and their corresponding variances). In the context of this study, PCs can be seen envisioned as aortic shape modulators changing a shape within a specific section of the aorta.

Sampled and preprocessed aortic centerline curves yielded a system coordinate vector $\mathbf{v_n}$, $n \in [1, 93]$ representing patient n specific aortic centerline. These patient-specific row vectors $\mathbf{v_n} = [\mathbb{x}, \mathbb{y}, \mathbb{z}]$ were uniformly arranged to contain a set of Cartesian coordinates for each point along the centerline arranged by each coordinate axis such as $\mathbb{x}_n = [(x_{n,1}, x_{n,2}, \ldots x_{n,100}]$, $\mathbb{y}_n = [y_{n,1}, y_{n,2}, \ldots y_{n,100}]$, and $\mathbb{z}_n = [z_{n,1}, z_{n,2}, \ldots z_{n,100}]$ filling into n-by-m matrix

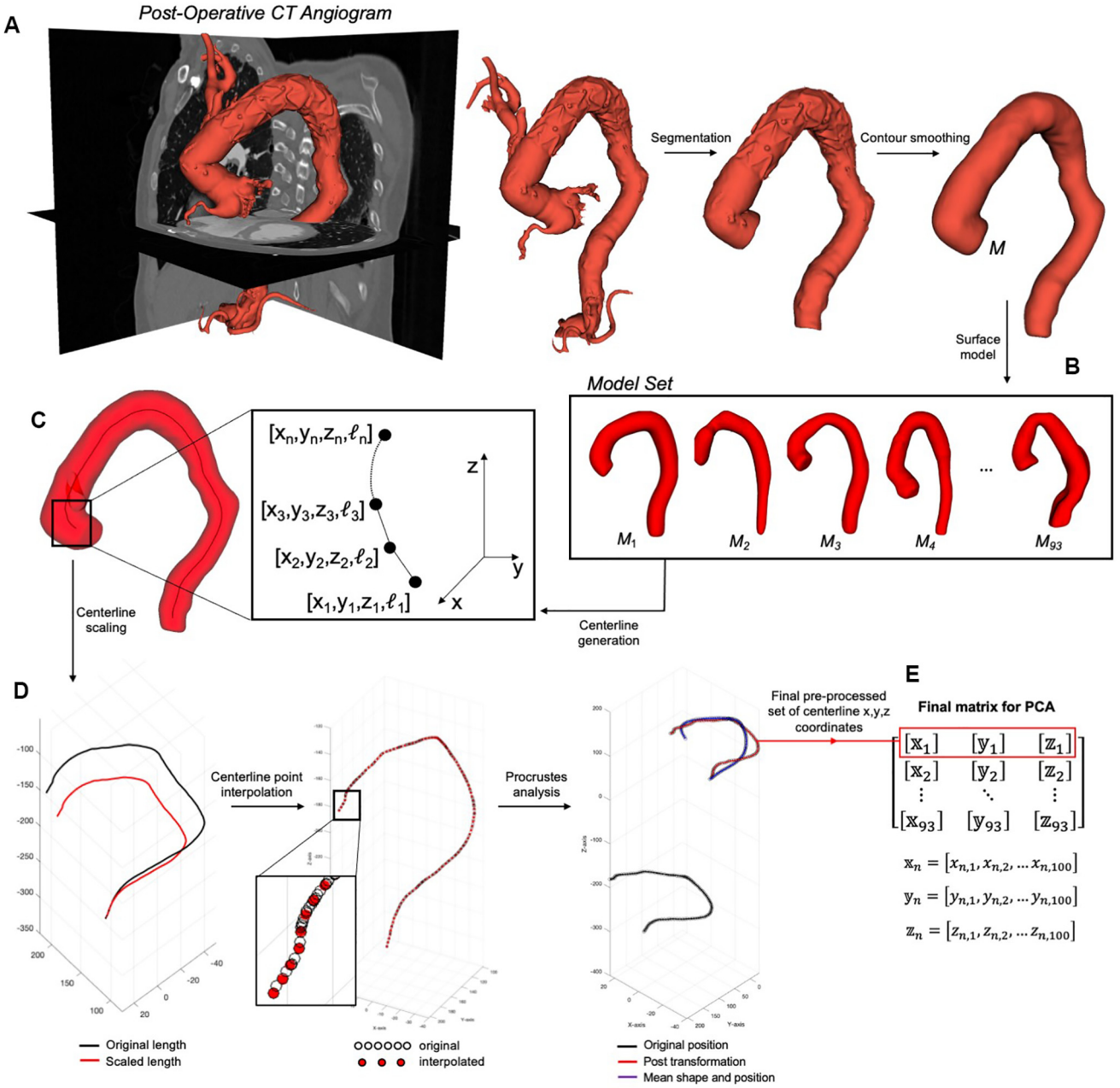

FIGURE 1. Work process depicting the aortic segmentation and preprocessing for the PCA. A, Computed tomography angiogram obtained before discharge was used to derive semiautomatically delineated aortic contours that further underwent standardized segmentation involving removing aortic/graft branches, defining the proximal and distal ends of the contour, and smoothing. B, Delineated contours were then used to build a surface model that was then subjected to centerline analysis (C) yielding a set of principal Cartesian coordinates (x, y, and z) and corresponding curve length-distance from the origin of the curve (L). D, Thereafter, aortic centerlines were preprocessed using sequential steps involving length scaling, data point interpolation, and Procrustes analysis. E, Final preprocessed set of coordinates served as an input for the PCA. *CT,* Computed tomography; *PCA*, principal component analysis.

$$\mathbb{M}_{n\times m} = \begin{bmatrix} - & \mathrm{v}_1 & - \\ - & \mathrm{v}_2 & - \\ - & \vdots & - \\ - & \mathrm{v}_n & - \end{bmatrix}$$

where $\mathbb{M}$ served as the final matrix for the PCA.

Given that $n < m$, PCA yielded 93 PC vectors $\mathbf{p}_n$, $n \in [1, 93]$ representing aortic shape modulators each with corresponding coefficients. The $\mathbf{p}_n$ vectors are describing the aortic shape modulation and are ranked by the proportion of their variance and accompanied by their corresponding set of aortic curvature PC score values s_n for each patient. These shape score values are scalar values representing a dot product between $\mathbf{p}_n$ and patient-specific aortic shape vector. To appreciate the effect of aortic shape modulators on average aortic shape $\bar{\mathbf{v}}$, we calculated a PC-specific shape deformation curves

$$\mathbf{v}_{\mathbf{def}}^{\mathbf{k}} = \bar{\mathbf{v}} + \mathrm{k}\bar{\mathbf{v}}\mathbf{p}_{\mathbf{n}}$$

where k represents a scaling factor k, k$\in\{-2,-1,0,1,2\}$ modulating the effect of the PC vectors.

Statistical Analysis

All statistical analyses and data presentation were performed with Prism (version 9.0 or higher; GraphPad Software Inc). All investigated variables were checked for the distributional assumption of normality using normal plots, in addition to D'Agostino-Pearson, Shapiro-Wilk, and Kolmogorov-Smirnov tests. Variables that were skewed were natural log transformed, and skewed variables that included negative values were natural log-modulus transformed for predictive analyses. Baseline demographic and clinical variables were reported as mean or median values with corresponding standard deviation or interquartile range, respectively, as dictated by the data distribution. Intergroup comparisons were performed using Student unpaired 2-tailed *t* test for normally distributed continuous variables or Mann–Whitney test for non-normally distributed variables, and chi-square or Fisher exact test for categorical variables.

PC scores were subjected to simple univariate logistic regression analysis and intergroup comparison to explore association with the aortic events defined as a composite of outcome including aortic rupture, new type B dissection, thoracoabdominal degeneration with persistent dissection, enlarging thoracic ascending aortic aneurysm, aortic root dissection or pseudoaneurysm, residual descending aortic dissection with residual FL flow, or TEVAR complications (endoleak, dissociation). Analyses were considered exploratory and hypothesis generating, and adjustments for multiple variable comparisons were not performed. Significance was based on an alpha value 0.05 or less.

RESULTS

Clinical characteristics and patient demographics are summarized in Table 1. Presenting diagnoses or indications for the FET procedure were in isolation or combination: TAAAD (n = 69, 74.2%), ascending aortic aneurysm with or without aortic valve insufficiency (n = 49, 52.7%), and isolated aortic arch pathologies (n = 6, 6.4%) including aneurysms, mycotic isolated rupture, or pseudoaneurysm. Twenty-one aortic events (22.6%) were encountered within a median 2.5-year follow-up and included aortic rupture (n = 1), new type B dissection (n = 4), symptomatic rapidly expanding thoracoabdominal aneurysm requiring open or endovascular repair (n = 5), residual descending dissection with persistent FL flow (n = 3), aortic root dissection or pseudoaneurysm (n = 3), enlarging arch/thoracic aortic aneurysm (n = 3), and TEVAR complications (n = 2). There were no differences in standard demographic parameters including age, sex distribution, and body mass index between patients with and without aortic events. Likewise, there were no differences between patients with and without the aortic event in the history of prior aortic pathology or presentation before the FET.

Principle Component Analysis

The results of the PCA are graphically summarized in Figure 2. Percent variance of aortic shapes described by individual PCs in descending order is depicted in Figure 2, *A*. The first 3 PCs accounted for 36.4%, 26.4%, and 11.6%, respectively, of aortic shape variance and cumulatively for 74.5% of the shape variation in all patients and were further considered for statistical analysis. The shape-modulating effect of the first 3 PCs on the aortic centerline is depicted in Figure 2, *B*, and further displayed explaining shape variations in Figure 3. The first PC (PC1), accounting for 36.4% of patient variability, described the variation of aortic arch height-to-length ratio. Specifically, shape modulation toward negative PC1 scores formed the aortic shape with low arch height-to-length ratio, and modulation toward positive PC1 scores produced the aortic shape with high arch height-to-length ratio. The second PC (PC2) described the aortic shape modulator altering variability of the aortic curve angle at the region of the aortic isthmus and to a minor

TABLE 1. Patient demographics and clinical characteristics

	All patients (N = 93)	No event (N = 72)	Aortic event (N = 21)	*P* value
Age (y)	60.2 (51.0-67.7)	59.9 (50.6-67.6)	60.4 (49.2-69.3)	.911
Sex (female)	25 (26.9%)	22 (30.5%)	3 (14.3%)	.170
BMI (kg/m^2)	27.9 (24.3-31.9)	28.1 (24.6-32.6)	26.4 (23.0-29.8)	.198
Aortic history				
Connective tissue disease	8 (8.6%)	4 (5.5%)	4 (19.0%)	.074
Aortic valve abnormality	29 (31.2%)	20 (27.7%)	9 (42.8%)	.283
Aortic root abnormality	27 (29.0%)	21 (29.2%)	6 (28.6%)	>.99
Prior aortic surgery	31 (33.3%)	23 (31.9%)	8 (38.1%)	.608
Presenting pathology				
TAAAD	69 (74.2%)	51 (70.8%)	18 (85.7%)	.257
Ascending or arch aneurysm	49 (52.7%)	40 (42.8%)	9 (55.5%)	.331
Additional procedure				
Aortic valve replacement	18 (19.3%)	15 (20.8%)	3 (14.3%)	.551
Aortic root replacement	35 (37.6%)	28 (38.9%)	7 (33.3%)	.799

Data are reported as median with corresponding IQR. *P* value represents unpaired 2-tailed Mann–Whitney or Fisher exact test. *BMI*, Body mass index; *TAAAD*, type A acute aortic dissection.

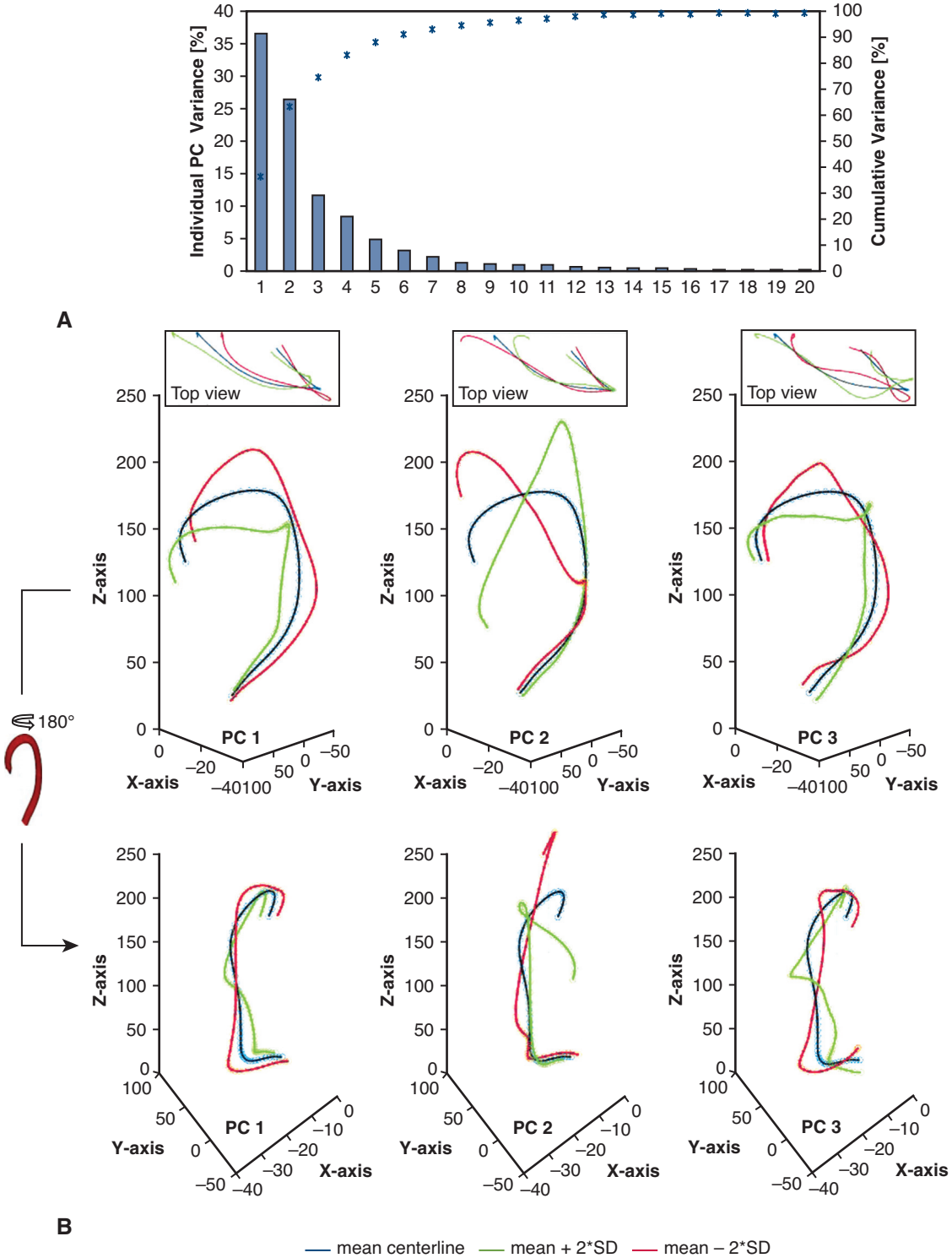

FIGURE 2. A, The scree plot with cumulative percent variance of observed PCs (only first 20 PCs are displayed). B, Three-dimensional representation of aortic centerline variation as dictated by observed PCs. *PC,* Principal component; *SD,* standard deviation.

degree a relative angle of the ascending aorta to the sinotubular junction. Specifically, PC2-positive scores described minimal angulation at the isthmus with the immediate downward turn of the aorta. PC2-negative scores described the acute angle at the region of isthmus and upward orientation of the aorta. The third PC (PC3)

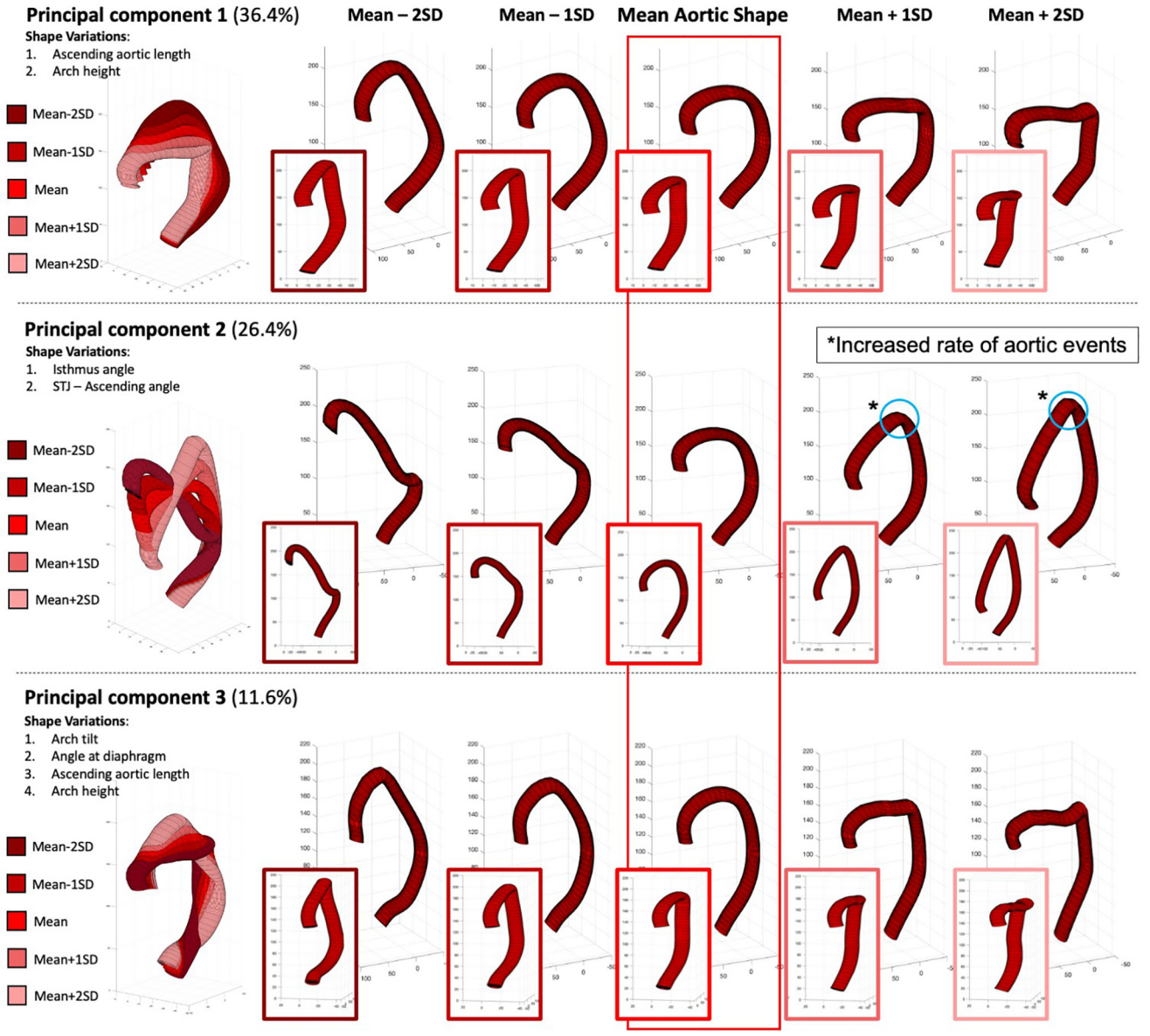

FIGURE 3. Described PCs with their effect on the overall aortic shape. *Top*: PC1, which modules the aortic shape by altering the ascending aortic length to arch height ratio. *Middle*: PC2-based aortic shape variations specifically describing the angle variation at the region of sinotubular junction and aortic isthmus. *Depicts aortic shape variations associated with the aortic events, with *blue circles* emphasizing the isthmus region with acute angle variation. *Bottom*: The effect of the PC3 on the aortic shape and specifically the variability in the aortic arch tilt and the insertion angle of the thoracoabdominal aorta with respect to the diaphragm. *SD,* Standard deviation.

described the variation of the arch tilt (anterior vs posterior) and the insertion of angle of the descending aorta to diaphragmatic hiatus. Positive PC3 values described the angulated/kinked portion of the thoracoabdominal aorta, whereas negative PC3 values described the straight segment.

Principal Components and Aortic Events

The simple univariable categorical regression analysis is summarized in Table 2. There was no association between PC1 scores describing the variation of aortic arch height-to-length ratio and the aortic events ($\beta \pm$ standard error [SE]: -0.002 ± 0.005, $P = .711$). PC2 describing the angle variation at the region of the aortic isthmus was associated with the aortic events ($\beta \pm$ SE: -0.012 ± 0.006, $P = .046$). Specifically, negative PC2 scores describing a tendency toward acute angle at the isthmus region were likely to be present in patients who experienced the aortic event (Figure 3). Last, there was no association between observed PC3 scores and aortic events ($\beta \pm$ SE: 0.002 ± 0.009, $P = .860$).

TABLE 2. Simple univariate logistic regression of principal components

	$\beta \pm$ SE	OR	95% CI	*P* value
PC1	0.002 ± 0.005	1.00	0.99-1.01	.711
PC2	−0.012 ± 0.006	0.98	0.97-0.99	.046
PC3	0.002 ± 0.009	1.00	0.98-1.02	.860

Data reported as beta coefficients with corresponding SE and OR. *SE,* Standard error; *OR,* odds ratio; *CI,* confidence interval; *PC,* principal component.

Projection of patient-specific scores on the first 2 PCs with categorical labeling of no event versus aortic event is depicted in Figure 4.

Intergroup comparison of individual PC scores between patients with no aortic event versus event group is summarized in Figure 5. There was no difference in observed scores between the considered groups for PC1 (−1.0 ± 47.2 vs 3.6 ± 63.1, $P = .724$) and PC3 (−0.3 ± 29.5 vs 0.9 ± 23.3, $P = .861$). PC2 scores describing the variation in the isthmus and sinotubular junction angles were higher in patients who experienced no aortic events (4.9 ± 42.7 vs −16.9 ± 39.1, $P = .038$).

DISCUSSION

Shape is a recognized aortic biomarker with a potential to predict clinical and hemodynamic events.[15,19,20] In the past, aortic shape has mostly been described using semiquantitative markers such as tortuosity, curvature index, tapering, or by qualitative descriptors such as Gothic, crenel, or Romanesque arch. Recently, more comprehensive approaches using statistical shape modeling and machine learning techniques have been used to predict global aortic remodeling, flow patterns, ventricular function, and clinical outcomes.[8,9,15] In this study, we describe aortic shape variations after the FET procedure using PCA and discovered that specific aortic shapes might be more prone to developing adverse aortic events. Specifically, shape type with the acute angulation at the region of the aortic isthmus was associated with subsequent aortic events independently of common preoperative risk factors. Further study is required to determine whether the shape is causal or a marker of the anatomic issues intrinsically prone to complications.

Although advancements have been made in FET surgical techniques, less progress has been made in reduction of long-term aortic complications. The mid- to long-term reports on incidence of aortic events after the FET vary in many studies ranging from approximately 16% to 47%.[5,21-24] This variability is mainly due to specifically selected patient cohorts under investigation and variable definitions of composite aortic events. Given the applicability of the FET procedure to many aortic pathologies, high incidence of distal aortic failure, and need for future aortic procedures, there is an urgent need for accurate predictors of aortic remodeling and adverse aortic events.[22-24] Furthermore, the FET procedure and its modified versions are increasingly more favored surgical approaches in the treatment of thoracic aortic disease in a younger patient population with tissue hereditary diseases, which translates to a lifetime of exposure and

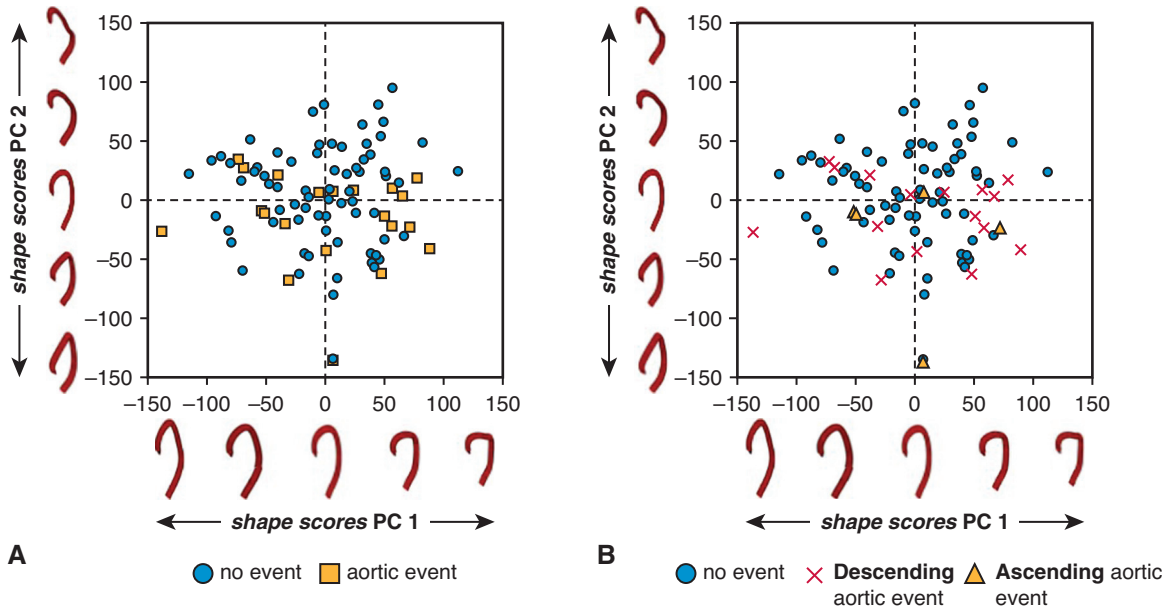

FIGURE 4. A, Individual patient aortic shape scores projected on the first and second PCs. One can appreciate that higher PC2 score values were more associated with patients who did not experience aortic events. B, Identical scatter plot with aortic events separated into ascending and descending aortic events. *PC*, Principal component.

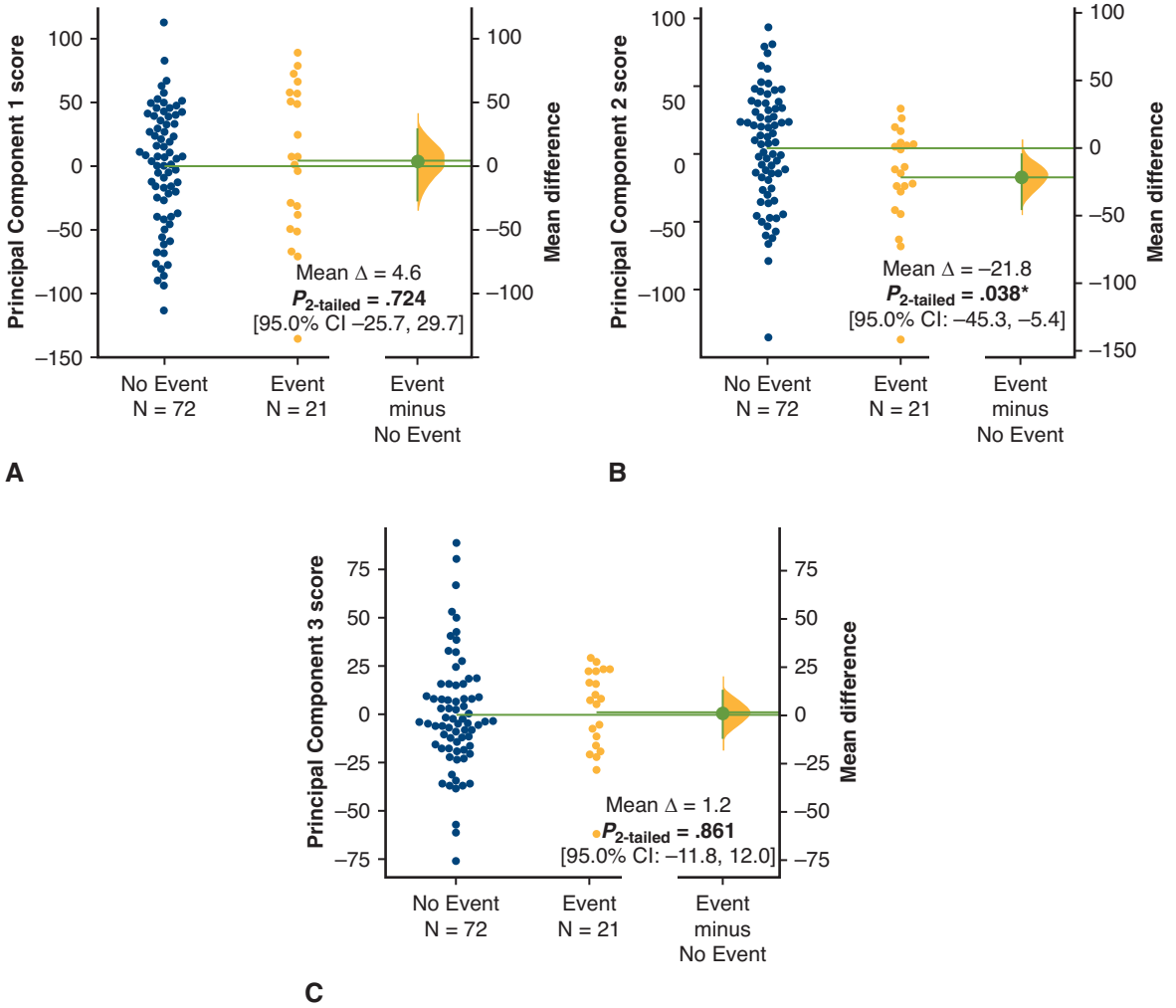

FIGURE 5. Graphical representation of the comparison of patient-specific PC scores for (A) PC1, (B) PC2, and (C) PC3 between patients with and without aortic events. PC2 scores representing shapes with more obtuse angle were significantly higher in patients with no aortic events. *CI,* Confidence interval.

increased long-term risk of aortic events. Current surveillance techniques describe aortic remodeling after the FET in terms of TL and FL size parameters or aortic growth rate.[4,6,23] Likewise, the most frequently assessed aortic predictors are aortic size parameters, with the preoperative maximum descending aortic diameter having the strongest potential to predict aortic events.[6,23,25]

The impetus for this evaluation came from the ideas that some patients have increased myocardial afterload after thoracic endovascular aortic repair or arch repair.[26,27] This spurred the thought that shape may play a role in addition to extent of repair. Better understanding of these principles may facilitate a more cardiac friendly repair. The presence of the stent-graft and acute angulations create a compliance mismatch resulting in additional backward wave reflections elevating myocardial afterload.[8,28] Acute angle variation at the region of the aortic isthmus or sinotubular junction described in this study by PC2 is a prominent feature of aortic shape post-FET. With the advent of FETs, the proximal position of the stented repair was distal to the left subclavian. Many surgeons have proximalized this stent for ease of repair, but the effect of this on the clinical outcomes and even the effect on the cardiac work are not known. This study is the initial foray into validating optimal shape of repair.

Clearly, there is direct interplay between the vessel shape and the resulting flow hemodynamics. Flow-mediated forces such as wall shear stress impacting aortic wall remodeling are inherently determined by the aortic shape and size.[29-31] Aortic shape postcoarctation repair or Norwood reconstruction is also associated with abnormal blood pressure response and backward traveling wave reflections elevating ventricular afterload.[8,16,28] Specifically, angulated Gothic arch has been described as a risk factor for developing long-term hemodynamic sequalae such as systemic hypertension. Unfortunately, similar

studies mainly exist in congenital patient populations, and investigations in adult thoracic aortic disease focusing on aortic shape postsurgical repair are missing. In our study, PC2 describing angulation at the region of the aortic isthmus was associated with composite aortic events. Presently, we do not know exactly what the biomechanical disadvantage role of this shape variation might be, but we plan to investigate this aortic variant in future studies using wave intensity analysis and flow imaging. The observed association was the only significant predictor of the aortic events in contrast to the presence of connective tissue disease and the TAAAD diagnosis, 2 recognized strong predictors of postoperative complications.[3] Our current practice technique is to create a proximal stent-graft fenestration to alleviate mechanical tensile and flow-mediated wall shear stress at the region of the isthmus-descending thoracic aorta.

The PCA and statistical shape analyses have been used in aortic investigations before. An interesting prospective study by Williams and colleagues[15] evaluated native aortic shape in patients serially followed for ascending thoracic aortic aneurysm using PCA of the 3-dimensional deformation matrix of the thoracic aorta. The authors identified the PC associated with aortic tortuosity, size, and ascending:-descending size ratio, which approached statistical significance when predicting the chance of developing TAAAD. This exciting novel approach might significantly aid with the surveillance and risk assessment in patients diagnosed with ascending thoracic aortic aneurysms. Cosentino and colleagues[32] similarly investigated patients with ascending thoracic aortic aneurysms and described PCA-based model predicting the need for surgery, which superseded the baseline model based on maximum aortic diameter. A study focusing on flow hemodynamic–geometry interactions revealed mechanistic changes in the velocity patterns, blood pressure, and wall shear stress with changes in principal shape modes.[33] We plan to investigate the observed postsurgical shape changes in conjunction with flow-sensitive imaging techniques such as 4-dimensional flow and standard phase-contrast magnetic resonance imaging to further appreciate the effect on flow hemodynamics and wave propagation.

Study Limitations

We recognize several limitations pertinent to this study. First, this was a retrospective study that involved only patients with TAAAD or ascending aortic/arch aneurysm. These diagnoses represent a significant risk factor for postsurgical complications. Our future studies will focus on validation of observed association with aortic events by investigating patients who underwent different types of aortic surgery (hemiarch replacement, zone 2 arch replacement with stage endovascular repair). Second, our preprocessing of aortic contours involved removal of head and neck vessels and inclusion of TL only for the aortic segmentation. The positioning of arch vessels influences important physiologic events such as pressure wave reflections and flow hemodynamics.[31] As stated in the "Materials and Methods" section, we focused on TL segmentation to limit the shape variability that would occur in patients with residual patent communications or variable degree of FL thrombosis. In future studies, we will also focus on a more iterative shape analysis approach to the more easily standardized shorter segment of the thoracic aorta. Last, our study did not focus on aortic diameter variation along the aortic length. That parameter can be subjected to similar PCA analysis, but for the reasons described we decided to not pursue that investigation at this time. Overall, we consider our results preliminary and encourage replication of our findings in similar cohorts to assess the potential of aortic shape after the FET procedure to become a surveillance risk factor.

CONCLUSIONS

The complexity of aortic shape after FET repair can be evaluated using PCA. The PC2, describing angulation at the region of the aortic isthmus, was associated with adverse aortic events. Observed shape variation might aid in risk stratification for future aortic events and should be validated in patients with broader thoracic aortic disease diagnoses and in different surgical techniques. Future studies should evaluate observed shape variation in the context of aortic biomechanical properties and flow hemodynamics.

Conflict of Interest Statement

The authors reported no conflicts of interest.

The *Journal* policy requires editors and reviewers to disclose conflicts of interest and to decline handling or reviewing manuscripts for which they may have a conflict of interest. The editors and reviewers of this article have no conflicts of interest.

References

1. Kato M, Ohnishi K, Kaneko M, Ueda T, Kishi D, Mizushima T, et al. New graft-implanting method for thoracic aortic aneurysm or dissection with a stented graft. *Circulation*. 1996;94(9 Suppl):II188-93.
2. Evangelista A, Isselbacher EM, Bossone E, Gleason TG, Eusanio MD, Sechtem U, et al. Insights from the international registry of acute aortic dissection: a 20-year experience of collaborative clinical research. *Circulation*. 2018; 137:1846-60.
3. Malaisrie SC, Szeto WY, Halas M, Girardi LN, Coselli JS, Sundt TM, et al. 2021 the American Association for Thoracic Surgery expert consensus document: surgical treatment of acute type A aortic dissection. *J Thorac Cardiovasc Surg*. 2021;162:735-58.e2.
4. Iafrancesco M, Goebel N, Mascaro J, Franke UFW, Pacini D, Di Bartolomeo R, et al. Aortic diameter remodelling after the frozen elephant trunk technique in aortic dissection: results from an international multicentre registry. *Eur J Cardiothorac Surg*. 2017;52:310-8.
5. Ma WG, Zhang W, Zhu JM, Ziganshin BA, Zhi AH, Zheng J, et al. Long-term outcomes of frozen elephant trunk for type A aortic dissection in patients with Marfan syndrome. *J Thorac Cardiovasc Surg*. 2017;154:1175-89.e2.

6. Dohle D-S, Tsagakis K, Janosi RA, Benedik J, Kühl H, Penkova L, et al. Aortic remodelling in aortic dissection after frozen elephant trunk. *Eur J Cardiothorac Surg*. 2016;49:111-7.
7. Kozlov BN, Panfilov DS, Saushkin VV, Nasrashvili GG, Kuznetsov MS, Nenakhova AA, et al. Distal aortic remodelling after the standard and the elongated frozen elephant trunk procedure. *Interact Cardiovasc Thorac Surg*. 2019; 29:117-23.
8. Quail MA, Segers P, Steeden JA, Muthurangu V. The aorta after coarctation repair - effects of calibre and curvature on arterial haemodynamics. *J Cardiovasc Magn Reson*. 2019;21:1-9.
9. Bruse JL, Khushnood A, McLeod K, Biglino G, Sermesant M, Pennec X, et al. How successful is successful? Aortic arch shape after successful aortic coarctation repair correlates with left ventricular function. *J Thorac Cardiovasc Surg*. 2017;153:418-27.
10. Schäfer M, Di Maria MV, Jaggers J, Stone ML, Ivy DD, Barker AJ, et al. High-degree Norwood neoaortic tapering is associated with abnormal flow conduction and elevated flow-mediated energy loss. *J Thorac Cardiovasc Surg*. 2021;162: 1791-804.
11. Hori D, Kusadokoro S, Mieno N, Fujimori T, Shimizu T, Kimura N, et al. The effect of aortic arch replacement on pulse wave velocity after surgery. *Interact Cardiovasc Thorac Surg*. 2022;34:652-9.
12. Bollache E, Fedak PWM, van Ooij P, Rahman O, Malaisrie SC, McCarthy PM, et al. Perioperative evaluation of regional aortic wall shear stress patterns in patients undergoing aortic valve and/or proximal thoracic aortic replacement. *J Thorac Cardiovasc Surg*. 2018;155:2277-86.e2.
13. Oechtering TH, Hons CF, Sieren M, Hunold P, Hennemuth A, Huellebrand M, et al. Time-resolved 3-dimensional magnetic resonance phase contrast imaging (4D Flow MRI) analysis of hemodynamics in valve-sparing aortic root repair with an anatomically shaped sinus prosthesis. *J Thorac Cardiovasc Surg*. 2016;152:418-27.
14. François CJ, Markl M, Schiebler ML, Niespodzany E, Landgraf BR, Schlensak C, et al. Four-dimensional, flow-sensitive magnetic resonance imaging of blood flow patterns in thoracic aortic dissections. *J Thorac Cardiovasc Surg*. 2013;145:1359-66.
15. Williams JG, Marlevi D, Bruse JL, Nezami FR, Moradi H, Fortunato RN, et al. Aortic dissection is determined by specific shape and hemodynamic interactions. *Ann Biomed Eng*. 2022;50:1771-86. https://doi.org/10.1007/s10439-022-02979-0
16. Ou P, Celermajer DS, Raisky O, Jolivet O, Buyens F, Herment A, et al. Angular (gothic) aortic arch leads to enhanced systolic wave reflection, central aortic stiffness, and increased left ventricular mass late after aortic coarctation repair: evaluation with magnetic resonance flow mapping. *J Thorac Cardiovasc Surg*. 2008; 135:62-8.
17. Eldeiry M, Aftab M, Bergeron E, Pal J, Cleveland JC, Fullerton D, et al. The Buffalo trunk technique for aortic arch reconstruction. *Ann Thorac Surg*. 2019;108: 680-6.
18. Fedorov A, Beichel R, Kalpathy-Cramer J, Finet J, Fillion-Robin JC, Pujol S, et al. 3D slicer as an image computing platform for the quantitative imaging network. *Magn Reson Imaging*. 2012;30:1323-41.
19. Quail MA, Knight DS, Steeden JA, Taelman L, Moledina S, Taylor AM, et al. Noninvasive pulmonary artery wave intensity analysis in pulmonary hypertension. *Am J Physiol Heart Circ Physiol*. 2015;308:H1603-11.
20. Bruse JL, Cervi E, McLeod K, Biglino G, Sermesant M, Pennec X, et al. Looks do matter! Aortic arch shape after hypoplastic left heart syndrome palliation correlates with cavopulmonary outcomes. *Ann Thorac Surg*. 2017;103:645-54.
21. Uchida N, Katayama A, Tamura K, Sutoh M, Kuraoka M, Murao N, et al. Long-term results of the frozen elephant trunk technique for extended aortic arch disease. *Eur J Cardiothorac Surg*. 2010;37:1338-45.
22. Berger T, Graap M, Rylski B, Fagu A, Gottardi R, Walter T, et al. Distal aortic failure following the frozen elephant trunk procedure for aortic dissection. *Front Cardiovasc Med*. 2022;9:911548.
23. Chen Y, Ma WG, Zhi AH, Lu L, Zheng J, Zhang W, et al. Fate of distal aorta after frozen elephant trunk and total arch replacement for type A aortic dissection in Marfan syndrome. *J Thorac Cardiovasc Surg*. 2019;157:835-49.
24. Ius F, Fleissner F, Pichlmaier M, Karck M, Martens A, Haverich A, et al. Total aortic arch replacement with the frozen elephant trunk technique: 10-year follow-up single-centre experience. *Eur J Cardiothorac Surg*. 2013;44:949-57.
25. Hiraoka A, Iida Y, Furukawa T, Ueki C, Miyake K, Mieno M, et al. Predictive factors of distal stent graft-induced new entry after frozen elephant trunk procedure for aortic dissection. *Eur J Cardiothorac Surg*. 2022;62:325.
26. Orihashi K. A simplified assessment of increased afterload by thoracic endovascular aortic repair. *JTCVS Tech*. 2020;1:11-3.
27. Quail MA, Short R, Pandya B, Steeden JA, Khushnood A, Taylor AM, et al. Abnormal wave reflections and left ventricular hypertrophy late after coarctation of the aorta repair. *Hypertension*. 2017;69:501-9.
28. Schäfer M, Frank BS, Jacobsen R, Rausch CM, Mitchell MB, Jaggers J, et al. Patients with Fontan circulation have abnormal aortic wave propagation patterns: a wave intensity analysis study. *Int J Cardiol*. 2021;322:158-67.
29. Guzzardi DG, Barker AJ, van Ooij P, Malaisrie SC, Puthumana JJ, Belke DD, et al. Valve-related hemodynamics mediate human bicuspid aortopathy. *J Am Coll Cardiol*. 2015;66:892-900.
30. Stalder AF, Russe MF, Frydrychowicz A, Bock J, Hennig J, Markl M. Quantitative 2D and 3D phase contrast MRI: optimized analysis of blood flow and vessel wall parameters. *Magn Reson Med*. 2008;60:1218-31.
31. Shalhub S, Schäfer M, Hatsukami TS, Sweet MP, Reynolds JJ, Bolster FA, et al. Association of variant arch anatomy with type B aortic dissection and hemodynamic mechanisms. *J Vasc Surg*. 2018;68:1640-8.
32. Cosentino F, Raffa GM, Gentile G, Agnese V, Bellavia D, Pilato M, et al. Personalized medicine statistical shape analysis of ascending thoracic aortic aneurysm: correlation between shape and biomechanical descriptors. *J Pers Med*. 2020;10: 28.
33. Catalano C, Agnese V, Gentile G, Raffa GM, Pilato M, Pasta S. Atlas-based evaluation of hemodynamic in ascending thoracic aortic aneurysms. *Appl Sci*. 2022; 12:394.

Key Words: sorta, frozen elephant trunk, principal component analysis, shape